Reply to Reviewers

Dear reviewers,

We would like to sincerely express our gratitude again for you taking the time and efforts to review our manuscript entitled "**Spatiotemporally consistent global dataset of the GIMMS Leaf Area Index (GIMMS LAI4g) from 1982 to 2020**" (essd-2023-68) submitted to *Earth System Science Data*. We have carefully considered all the comments and incorporated most of the suggestions, which have further improved the manuscript. We hope that the new version of the manuscript has addressed all the concerns.

Below we provide point-to-point responses, each following the specific comment from the reviewer. All the changes in the revised manuscript have been marked in red.

Sincerely yours,

Zaichun Zhu, Ph. D. (on behalf of the author team)

School of Urban Planning and Design

Peking University

Tel: 86 185 0042 6608

Email: zhu.zaichun@pku.edu.cn

Referee 1

[Comment 1] *I appreciate the authors adding new and supportive results to the new manuscript. The current version of the manuscript and the dataset has been substantially improved. There are only a few minor points for the authors to improve their manuscript.*

[Response 1] We thank all the constructive comments from the reviewer. We hope the minor points have been well addressed in this updated version of the manuscript.

[Comment 2] *1. The method used the consolidation with reprocessed MODIS LAI at the MODIS-era, so the trend after 2000 should be highlighted that it is depended on the trend from MODIS. The LAI trend after 2000 is not only from Landsat and AVHRR but also MODIS, which is an important point that should be pointed out in the abstract.*

[Response 2] Thanks for this suggestion. In the Abstract of the updated manuscript, we have now stated that "The consolidation with the reprocessed MODIS LAI allows the GIMMS LAI4g to extend the temporal coverage from 2015 to recent (2020), producing the LAI trend that maintains high consistency before and after 2000 and aligns with the MODIS LAI trend during the MODIS era." (Page 2, Lines 30-32).

[Comment 3] *2. I would also thank the author pay attention to the LAI trend analysis between pre-MODIS era and MODIS era. However, I think the results may not right. Particularly, the EBF could not have a decreasing trend at the pre-MODIS era. This may because of the AVHRR or Landsat data have limitation at the first a few years of observation. Moreover, for the trend analysis at the MODIS era, I recommend using the LAI data after 2003. The authors may refer to Yuan et al. (2011). So for the LAI trend analysis at the pre-MODIS era and MODIS era, it should be corresponded to 1984-1999 and 2003-2020, respectively.*

Yuan, H., Dai, Y., Xiao, Z., Ji, D., & Shangguan, W. (2011). Reprocessing the MODIS Leaf Area Index products for land surface and climate modelling. Remote Sensing of Environment, 115(5), 1171-1187.

Ref doc link: http://globalchange.bnu.edu.cn/research/laiv061

[Response 3] We admire the reviewer's incisive comment on the decreasing trend of EBF in the pre-MODIS era (before 2000) for GIMMS LAI4g. We find that the reason, as pointed out by the reviewer, is a combination of limitations in the AVHRR and Landsat data. The GIMMS LAI4g was based on the AVHRR/NOAA-7 data from January 1982 to February 1985. Meanwhile, the Landsat LAI samples have been absent before 1984 and were scarce in 1984 (3500 per biome on average and 620 for EBF) (Figure 2b). To address this issue, we have applied the version of BNPP models with explanatory variables of PKU GIMMS NDVI, spatial information, and temporal information only (i.e., NOAA satellite number and years since launch excluded) on the period of 1982−1984 for all vegetation biomes. It should be noted that, this version of BNPP models (R^2: 0.95; RMSE: 0.46 m^2/m^2; MAE: 0.27 m^2/m^2; MAPE: 12.27%) only showed slightly lower accuracies than the one used before (R^2: 0.95; RMSE: 0.45 m^2/m^2; MAE: 0.27 m^2/m^2; MAPE: 11.98%) (Figure 3). The abnormal decreasing trend of EBF in the pre-MODIS era has now been amended (Figure 13).

On the other hand, the division of pre- and post-MODIS era in this study was determined not only by the MODIS data used in GIMMS LAI4g (the Reprocessed MODIS LAI; 2004−2020), but also by those used in other LAI products. For instance, both GLASS LAI (version 4) and GLOBMAP LAI (version 3) used MODIS surface reflectance since 2000. To better compare the temporal consistency before and after the MODIS era for different LAI products, we have to compromise between the MODIS data and finally chose 2000 as the dividing year. We hope the reviewer understands our rationale.

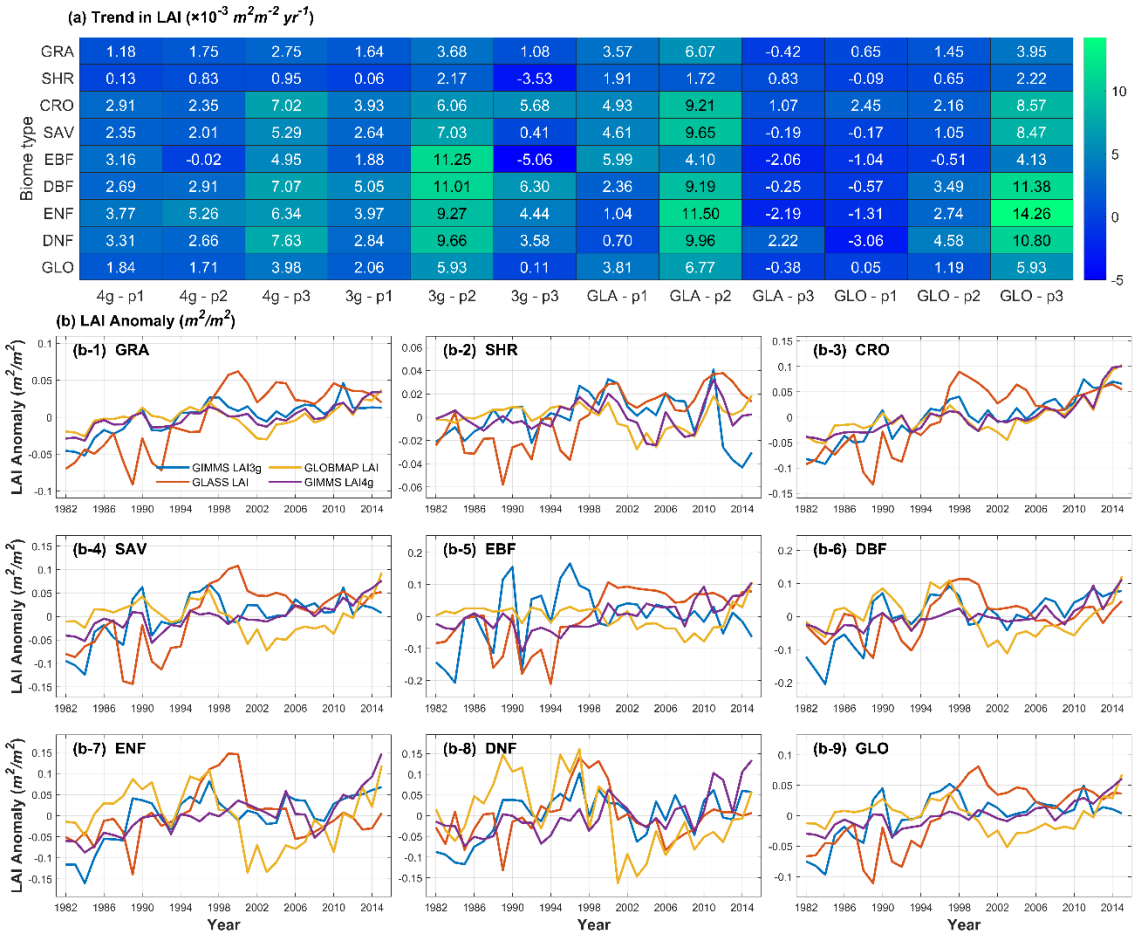

Figure 13. Variations of annual LAI anomaly of different vegetation biomes in the global LAI products during 1982−2015. The LAI products include GIMMS LAI4g, GIMMS LAI3g, GLASS LAI, and GLOBMAP LAI. (a) shows the slope values of the annual LAI during 1982−2015 (p1), 1982−2000 (p2), and 2001−2015 (p3). In the x-axis, 4g, 3g, GLA, and GLO stands for GIMMS LAI4g, GIMMS LAI3g, GLASS LAI, and GLOBMAP LAI, respectively. (b) shows the annual LAI time series.

The following changes are made in the revised manuscript:

• Results in determining the optimum BPNN models in Section 4.2:

"As such, for most periods during 1982−2015, the BPNN models adopted the combination of all explanatory variables (S5), including NDVI, longitude, latitude, month, NOAA satellite number, and NOAA satellite in orbit duration. For the period of 1982−1984, the BPNN models adopted the combination of NDVI, longitude, latitude, and month (S3) because of the acceptable accuracies (Figure 3 and Table 1) and the absence (before 1984)

and scarce (1984) Landsat LAI samples (see section 4.1) which could lead to a biased derivation of LAI." (Page 15, Lines 346-350)

• Discussions on the uncertainty source of GIMMS LAI4g product in Section 5.3:

"Also, the Landsat LAI samples were absent before 1984 and scarce in 1984 (section 4.1), which would produce larger uncertainties for the GIMMS LAI4g product during the NOAA-7 period (July 1981 to February 1985)." (Page 29, Lines 580-582)

[Comment 4] *Besides, there are two types of EBF, one is in tropical and the other one is in temperate region. To my humble knowledge, I think the tropical EBF could not have high LAI increasing rate because of the VPD stress (Yuan et al. 2019). Thus, the authors may also analysis the LAI trend at Amazon and Congo basin as the typical LAI trend of EBF at tropical region.*

Yuan, W., Zheng, Y., Piao, S., Ciais, P., Lombardozzi, D., Wang, Y., ... & Yang, S. (2019). Increased atmospheric vapor pressure deficit reduces global vegetation growth. Science advances, 5(8), eaax1396.

[Response 4] We thank the reviewer for raising this point, which helps us further improve our data in the important EBF ecosystems. Similar to **Comment 3/Response 3**, we also find limited Landsat LAI samples in EBF from October to April, especially for the years 2012 and 2013 (Figure 2b; Section 4.1). During this period, the scarce Landsat LAI samples had led to an overestimated greening trend for GIMMS LAI4g after 2000. Therefore, in EBF we have also adopted the version of BNPP models without explanatory variables of NOAA satellite number and years since launch, for all periods of October to April during 1982−2015. The high LAI increasing rate in EBF of GIMMS LAI4g has disappeared, and the trend is more reasonably consistent compared to other products (Figure 13).

To further investigate the LAI trends at Amazon and Congo basins, we have analyzed the LAI anomalies using GIMMS LAI4g before consolidation (1982−2015), GIMMS LAI4g after consolidation (1982−2020), GIMMS LAI3g (1982−2015), GLASS LAI (1982−2015), and GLOBMAP LAI (1982−2015), as shown in Figure S16.

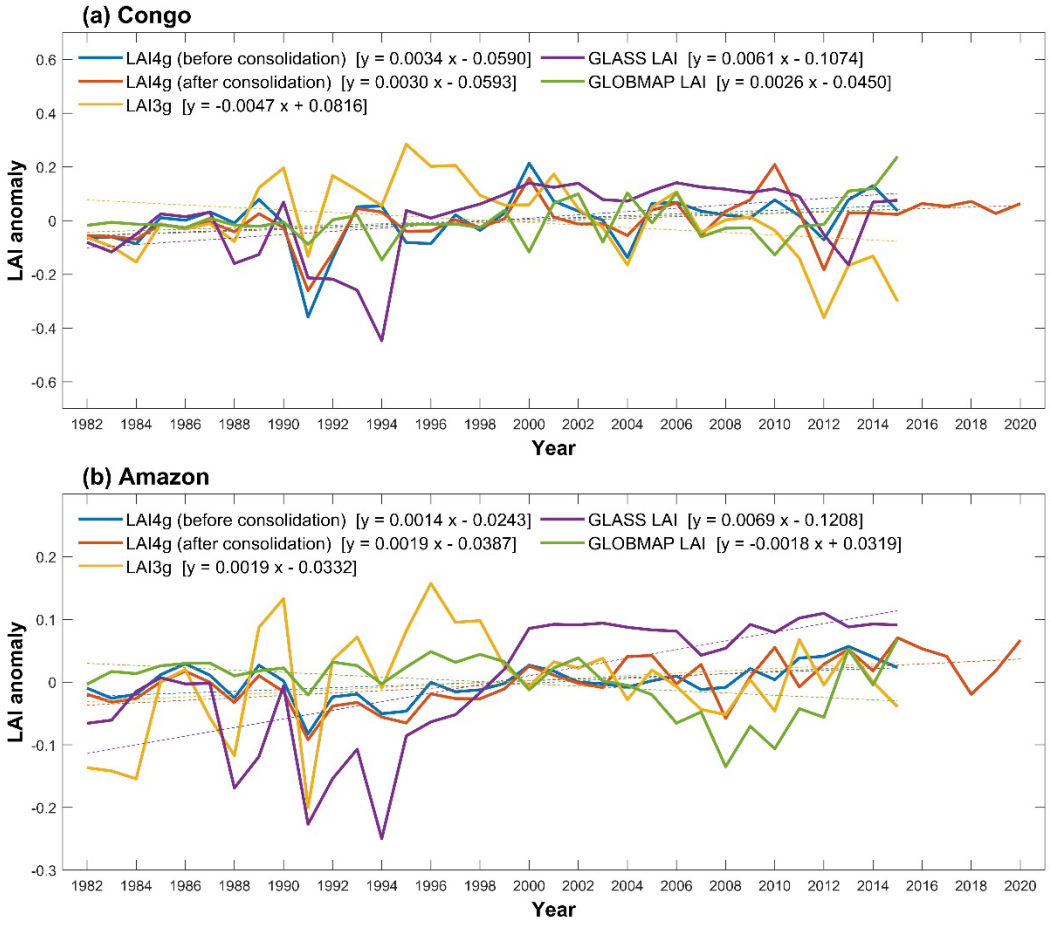

Figure S16. Annual anomalies (m^2m^{-2}) and trends of GIMMS LAI4g before consolidation (1982−2015), GIMMS LAI4g after consolidation (1982−2020), GIMMS LAI3g (1982−2015), GLASS LAI (1982−2015), and GLOBMAP LAI (1982−2015) in the Congo (a) and Amazon (b) forests.

All the products presented a greening trend in the Congo forests except the GIMMS LAI3g (-4.7×10^{-3} $m^2m^{-2}yr^{-1}$), with GLASS LAI (6.1×10^{-3} $m^2m^{-2}yr^{-1}$) presenting the largest slope, followed by GIMMS LAI4g (before consolidation: 3.4×10^{-3} $m^2m^{-2}yr^{-1}$; after consolidation: 3.0×10^{-3} $m^2m^{-2}yr^{-1}$) and GLOBMAP LAI (2.6×10^{-3} $m^2m^{-2}yr^{-1}$). In the Amazon forests, the GIMM LAI4g before (1.4×10^{-3} $m^2m^{-2}yr^{-1}$) and after consolidation (1.9×10^{-3} $m^2m^{-2}yr^{-1}$), GLASS LAI (6.9×10^{-3} $m^2m^{-2}yr^{-1}$), and GIMMS LAI3g (1.9×10^{-3} $m^2m^{-2}yr^{-1}$), had a greening trend while the GLOMAP LAI had a browning trend (-1.8×10^{-3} $m^2m^{-2}yr^{-1}$). Therefore, in the updated version of GIMMS LAI4g, both the Congo and Amazon basins showed moderate but persistent green trends.

The following changes are made in the revised manuscript:

- Results in determining the optimum BPNN models in Section 4.2:

"Similarly, S3 was also adopted in the winter of ENF (Northern Hemisphere: October to April; Southern Hemisphere: May to September) and October to April of EBF due to the limited Landsat LAI samples (Figure 2)." (Page 15, Lines 351-352)

- Results of LAI trend analysis in Section 4.5:

"We also paid attention to the vegetation trends in the EBF of Amazon and Congo (Figure S16). Large inconsistencies were found between the LAI products. Almost all the LAI products presented a greening trend except the GIMMS LAI3g in the Congo forests (-4.7×10^{-3} $m^2m^{-2}yr^{-1}$) and the GLOMAP LAI in the Amazon forests (-1.8×10^{-3} $m^2m^{-2}yr^{-1}$). The GIMMS LAI4g had moderate greening trends compared to other products." (Page 26, Lines 510-513)

[Comment 4] *3. The other point I want to point out for the LAI trend is, since figure 13 analyzes the LAI trend among PFT. It is not clear whether the PFT fraction will change from 1982-2020. Thus, I think the LAI trend among PFT only based on the pixels where PFT fraction is unchanged among the investigated years. For example, the authors may use the PFT fraction with unchanged pixels from MCD12Q1 land cover map. The LUH2 is also acceptable for getting the PFT unchanged pixels.*

Hurtt, G. C., Chini, L., Sahajpal, R., Frolking, S., Bodirsky, B. L., Calvin, K., ... & Zhang, X. (2020). Harmonization of global land use change and management for the period 850–2100 (LUH2) for CMIP6. Geoscientific Model Development, 13(11), 5425-5464.

[Response 4] In this study, the land cover map was derived from the MCD12Q1 product, with the type of each pixel determined as the most frequent PFT during 2001−2019. "The most frequent PFT" represents a balance between the sample size and sample quality for GIMMS LAI4g generation and validation. We decided not to employ unchanged pixels only, as they were insufficient in quantity and spatially unrepresentative. However, we agreed that a trend analysis based on unchanged pixels would be beneficial in the future to reveal the vegetation dynamics in those relatively undisturbed regions, despite being out of the scope of the current study.

• Discussions on the uncertainty source of GIMMS LAI4g product in Section 5.3:
"In addition, this study used a static global land cover map determined by the most frequent biome type within each grid between 2001 and 2019. This strategy could bring potential uncertainties yet represents a balance between the sample size and sample quality for GIMMS LAI4g generation and validation. When applying GIMMS LAI4g for vegetation trends analysis, a careful consideration of land cover change is suggested." (Page 29, Lines 589-592)

Referee 3

[Comment 1] *The authors have provided detailed revisions and explanations; however, there are still two major questions remaining:*

[Response 1] We apologize for the insufficient information provided in the last version of the manuscript, especially those related to the PKU GIMMS NDVI and Landsat LAI samples. We thank the reviewer for raising these issues again. In the following responses, we have tried our very best to elaborate as many details as we can. We hope all the issues have been addressed in the updated manuscript.

[Comment 2] *1. More information is needed regarding the PKU GIMMS NDVI (Li et al., in review) used for algorithm development: a) How was cross-calibration implemented for TM, ETM+, and OLI NDVI? b) Regarding the extraction of "massive high-quality Landsat NDVI samples" considering factors such as clouds, cloud shadows, water, snow, aerosol, and radiation performance, do you mean that these samples were screened out for the presence of these factors? c) Please provide more details on the "other explanatory variables" mentioned.*

[Response 2] We thank the reviewer for the detailed suggestions regarding the clarification of our method. Following the reviewer's suggestion, the following details have been complemented in the revised manuscript subject to the concerns (a), (b), and (c). These details are also available in Li et al. (in press) which has been recently accepted for publication in ESSD (https://doi.org/10.5194/essd-2023-1).

(a) In the cross-calibration between TM, ETM+, and OLI NDVI, we adopted the method from Berner et al. (2020) to calibrate TM and OLI NDVI to the ETM+ level via BPNN. 100,000 sample locations were randomly selected for each vegetation biome type from the MCD12Q1 (500 m resolution). 20 × 20 Landsat pixels (30 m resolution) were extracted at each sample center from TM, ETM+, and OLI images during the overlapping periods. The sample locations were then refined by removing those (1) with a high atmospheric opacity (information provided by Landsat products) and (2) where more than 10% of the 20 × 20 Landsat pixels have low quality. The low quality was determined by the cloud coverage in the associated Landsat scenes (> 80%), the clouds, cloud shadows, water, or snow judged by the CF Mask algorithm (Zhu et al., 2015), and implausibly high (>1) or extremely low (0.001) surface reflectance. NDVI was calculated and averaged from high-quality pixels at the remaining sample locations. The sample locations were divided into 80% for BPNN training and 20% for BPNN evaluation. In the BPNN model, the explanatory variables included the NDVI of TM or OLI, the image acquisition time (day of the year), and the sample location's spatial coordinates (longitude and latitude). The target variable was the NDVI of ETM+.

(b) In the Landsat sample selection for generating the PKU GIMMS NDVI, we screened out samples that suffered from Mount Pinatubo eruption (August 1991 to December 1992), a high atmospheric opacity (information provided by Landsat products), and low quality. The quality of the sample was determined in the same way as in Landsat NDVI cross-calibration, i.e., a sample was considered as low-quality if most of the Landsat pixels were affected by clouds, cloud shadows, water, snow, aerosol, and implausible radiation performance.

(c) In training the BPNN model for PKU GIMMS NDVI, the explanatory variables for a particular sample include (1) its GIMMS NDVI3g value, (2) the longitude and latitude of the location, (3) the month that the sample belongs, (4) the NOAA satellite number that the GIMMS NDVI3g data was acquired from, and (5) years since the NOAA satellite launched. To this end, the "other explanatory variables" are the longitude and latitude, the month, and the NOAA satellite number and years since its launch.

In the updated manuscript, all the mandatory information of the abovementioned details has been added. However, we also compromise a few details to avoid possible repetition with the original paper (Li et al., 2023).

The following changes are made in the revised manuscript:

- Introduction to PKU GIMMS NDVI in Section 2.1:

"In the generation of PKU GIMMS NDVI, Landsat NDVI from Thematic Mapper (TM), Enhanced Thematic Mapper Plus (ETM+), and Operational Land Imager (OLI) were first cross-calibrated by adjusting the TM and OLI NDVI to the ETM+ level via random sample locations and the BPNN model (Berner et al., 2020). The sample locations were refined by removing those with high atmospheric opacity and low quality which was defined by the occurrence of clouds, cloud shadows, water, or snow and implausible radiation performance. In the BPNN model, the explanatory variables included the NDVI of TM or OLI, the image acquisition day of the year, and the sample location's longitude and latitude; and the target variable was the NDVI of ETM+.

After cross-calibration, massive high-quality Landsat NDVI samples were extracted by screening out samples that suffered from the Mount Pinatubo eruption (August 1991 to December 1992) as well a high atmospheric opacity and a bad quality (same as sample screening in cross-calibration). The Landsat NDVI samples were employed to calibrate the GIMMS NDVI3g product with other explanatory variables (the longitude and latitude, NDVI month, and NOAA satellite number and years since its launch) using biome-specific machine learning models." (Page 4, Lines 105-116)

[Comment 3] *The same issue arises with Landsat LAI samples. In line 120, "Biome- and Landsat sensor-specific Random Forest models with other explanatory variables were built based on the sample pairs." Please indicate what the explanatory variables are.*

[Response 3] In training the Random Forest model for the Landsat LAI sample dataset, the explanatory variables included Landsat surface reflectance, spectral indices (NDVI, NDWI, and EVI), the longitude and latitude of the sample, and solar zenith and azimuth

angles at the sample location. Therefore, the "other explanatory variables" are spectral indices, the longitude and latitude, and the solar zenith and azimuth angles.

The following changes are made in the revised manuscript:

- Introduction to Landsat LAI sample dataset in Section 2.2:

"Biome- and Landsat sensor-specific Random Forest models with other explanatory variables (NDVI, Normalized Difference Water Index [NDWI], Enhanced Vegetation Index [EVI], the longitude and latitude, and the solar zenith and azimuth angles) were built based on the sample pairs." (Page 5, Lines 136-138)

[Comment 4] *2. Concerning the Landsat LAI samples used for model training and validation: a) The distributions of Landsat LAI samples in lower values (0-1) account for a very high percentage (Fig.2c), which does not guarantee "good representativeness". Please provide an explanation for this. b) Are the Landsat LAI samples used for validation and consistency evaluation independent in terms of geolocation and temporal coverage? Please clarify.*

[Response 4] For concern (a), it may look counter-intuitive that a majority of Landsat LAI samples were distributed in lower values of 0-1. However, this value distribution agreed well with existing global long-term LAI products (GIMMS LAI3g, GLASS LAI, and GLOBMAP LAI) where statistics were conducted based on all terrestrial vegetation pixels (Figure 2c). This could be further confirmed by the work of Ma and Liang (2022). When developing the GLASS 250-m LAI, they presented a similar LAI distribution pattern via their Figure 4c as below. The dominant low LAI values could be explained by a large portion of the low-LAI vegetation biomes on Earth (grassland, shrubland, and savanna), the non-growing seasons for vegetation biomes such as cropland and deciduous forests, and the snow cover in the winter.

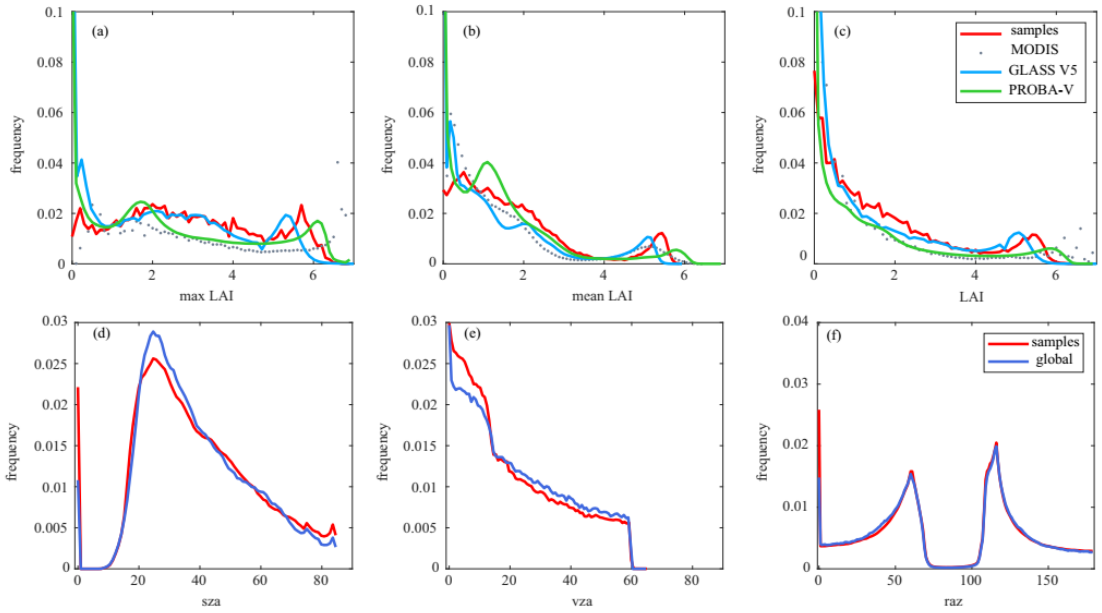

Fig. 4. Distribution of LAI values (bin width is 0.1) of the 2014–2015 time-series fused LAI samples at the representative pixels, and MODIS, PROBA-V, and GLASS V5 LAI at global land pixels: (a) "max LAI" represents the distribution of the maximum LAI values of the 2014–2015 LAI time-series, (b) "mean LAI" represents the distribution of the mean LAI values of the 2014–2015 LAI time-series, and (c) "LAI" represents the distribution of all the LAI values of the 2014–2015 time series; and distribution of (d) solar zenith, (e) view zenith and (f) relative azimuth angles (bin width is 1°) of the 2014–2015 time-series MODIS surface reflectance data at the representative pixels and the global land pixels.

For concern (b), we randomly divided the Landsat LAI sample dataset into 80% for BPNN model training and 20% for LAI product evaluation (the second paragraph in Section 3.1). Thus, these two groups of samples were independent of each other in terms of geolocation and temporal coverage. In this study, the evaluation group of Landsat LAI samples (20%) was used for both validation and consistency evaluation.

To avoid confusion, the following changes are made in the revised manuscript:

- In Figure 2 caption:

"For GIMMS LAI3g, GLASS LAI, and GLOBMAP LAI, the value distribution was calculated based on all terrestrial vegetation pixels." (Page 12, Lines 327-328)

[Comment 5] *Minor comments:*

1. In line 210, please describe how the MODIS LAI samples were selected.

[Response 5] When training the BPNN model, we found that the Landsat LAI sample size could be limited in certain locations and months (Figure 2a and Figure 2b). This is especially true for the northern mid-high latitudes in the winter due to the polar night

phenomenon and low solar altitude angle, which means that low LAI values have been lacking in the Landsat LAI samples for some vegetation biome types (i.e., grassland, shrubland, savanna, and ENF; see Figure 2a and Figure S3). To make the biome-specific BPNN models more accountable, we randomly selected 40,000 MODIS LAI samples at latitudes > 25° N in the winter months (October to April), 10,000 for each of the four vegetation biomes (grassland, shrubland, savanna, and ENF). It should be noted that evergreen broadleaf forests in the tropics did not suffer from the LAI values bias due to their consistently high LAI values across the year.

The following changes are made in the revised manuscript:

- BPNN model establishment in the second paragraph of section 3.1:

"Specifically, 10,000 Reprocessed MODIS LAI values were randomly introduced for each of GRA, SHR, SAV, and ENF at latitudes > 25° N in the winter months (October to April)." (Page 9, Lines 230-231)

[Comment 6] *2. In Figure 11, please explain why the trend of GIMMS LAI4g is different from the MODIS LAI in slopes after consolidation. Readers may be confused, as the GIMMS LAI4g has already been matched with the MODIS LAI product using the pixel-wise fusion method.*

[Response 6] Thanks for this comment. In Figure 11, the trend of GIMMS LAI4g after consolidation and that of MODIS LAI were calculated based on different periods. For GIMMS LAI4g after consolidation, the period was 1982-2020; and for the MODIS LAI, the period was 2004−2020. They were thus not comparable. We apologize for the confusion in the figure, which has been clarified in the updated version of the manuscript.

In fact, the slope of GIMMS LAI4g after consolidation during 2004−2020 had the same value (0.0056) as the MODIS LAI. In Figure 11, a very similar LAI anomaly pattern during 2004−2020 could be found between GIMMS LAI4g after consolidation and the Reprocessed MODIS LAI.

The following changes are made in the revised manuscript:

• In Figure 11 caption:

"Note that the regression equations within the square brackets were calculated from different periods depending on the products." (Page 24, Lines 486-487)

[Comment 7] *3. The previous comment on "Providing global distribution maps of GIMMS LAI4g at representative time points and comparing them with other products may be useful and informative for potential users" has not been addressed. I suggest adding the global LAI distribution maps, similar to the global land cover map in Figure S3.*

[Response 7] Thank you for raising this issue again. We sincerely apologize for this omission. In the previous version of the manuscript, only LAI variation curves at representative time points were added (Figure 7). We have now provided global distribution maps of GIMMS LAI4g in January and July of the years 1990 (Figure S4), 2000 (Figure S5), and 2010 (Figure S6), with a similar form as Figure S3 in the updated supplementary file. We hope this issue has been addressed.

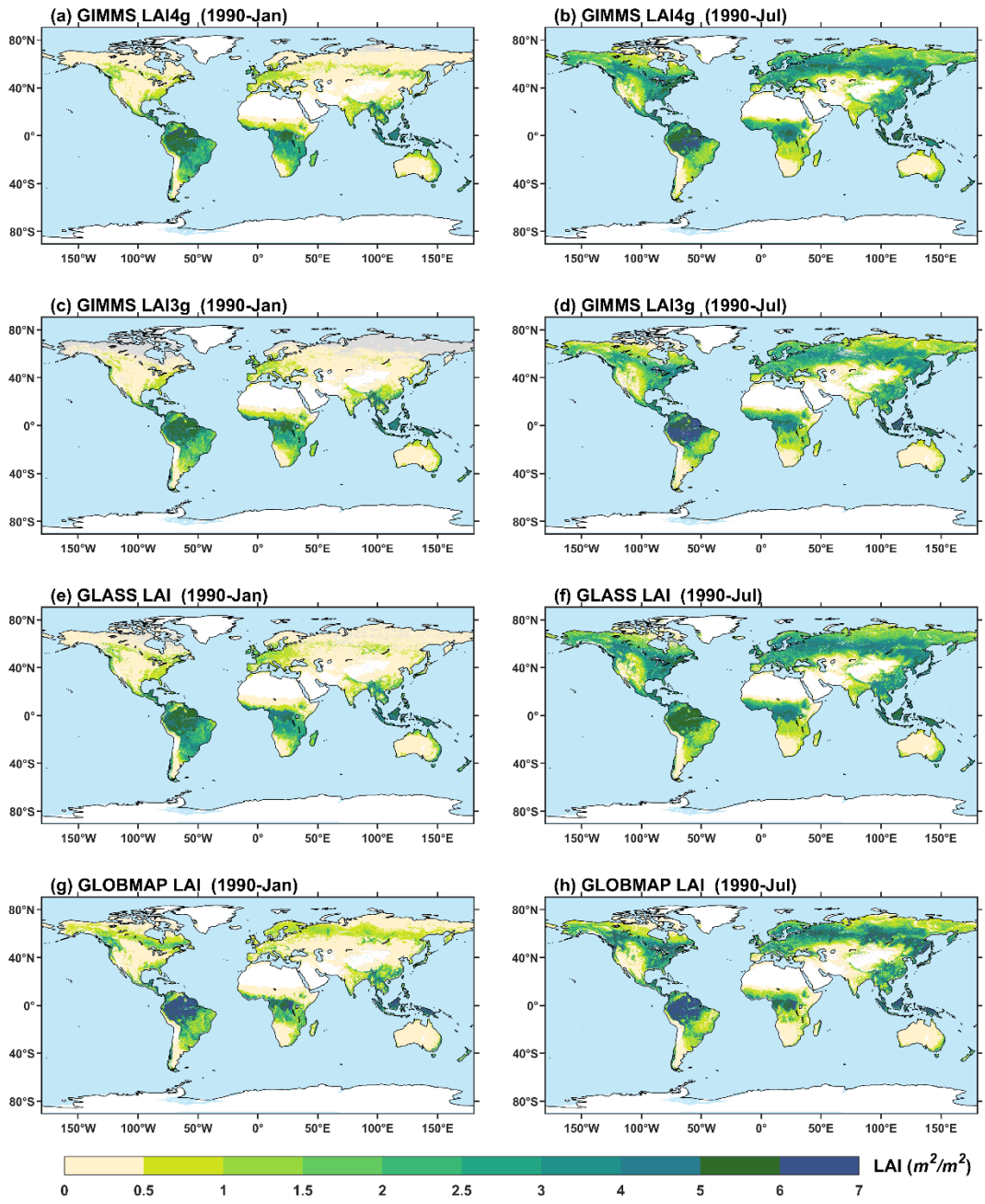

Figure S4. Illustrations of global distribution maps of GIMMS LAI4g after consolidation (a and b), GIMMS LAI3g (c and d), GLASS LAI (e and f), and GLOBMAP LAI (g and h) in January and July of **1990**.

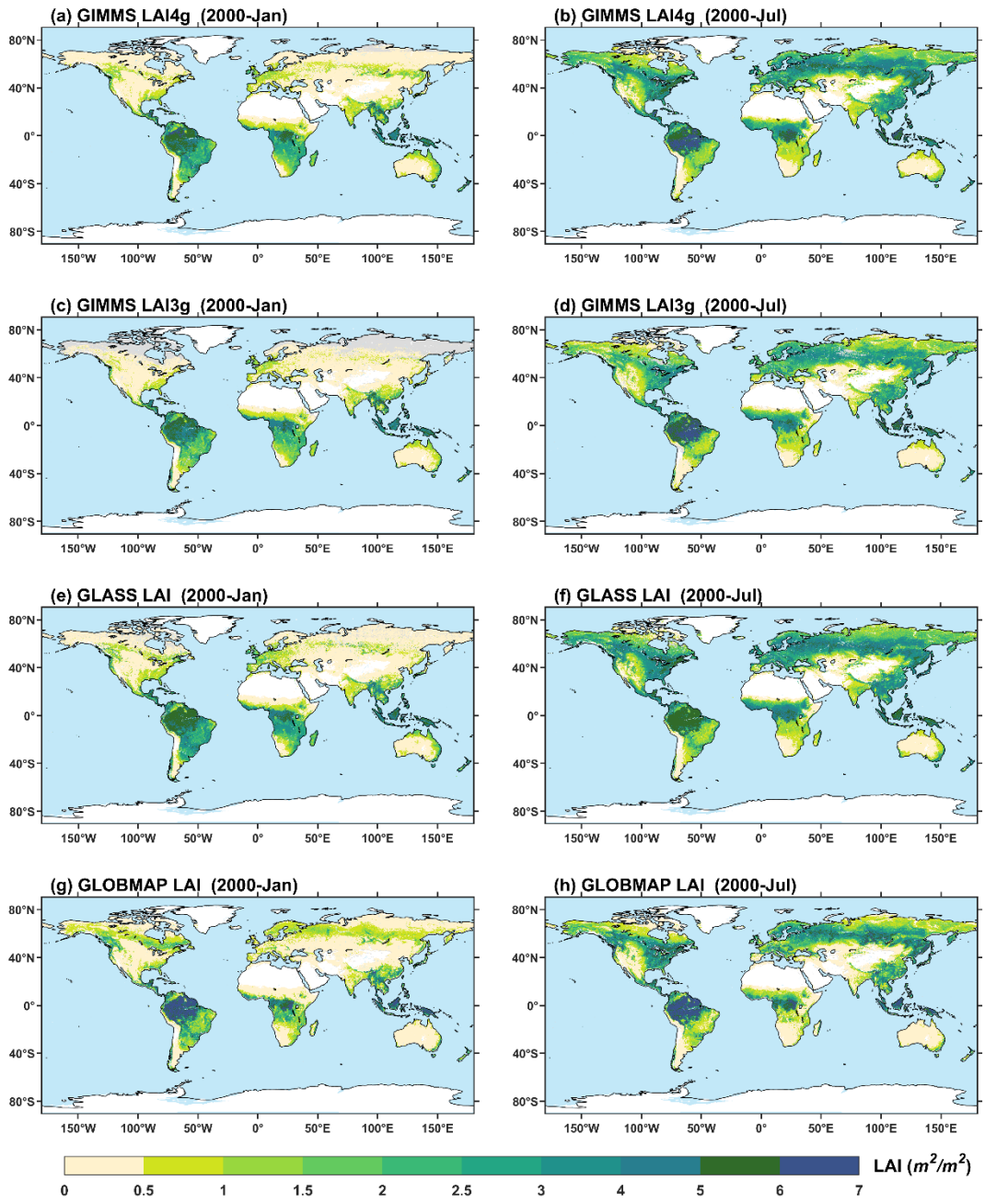

Figure S5. Illustrations of global distribution maps of GIMMS LAI4g after consolidation (a and b), GIMMS LAI3g (c and d), GLASS LAI (e and f), and GLOBMAP LAI (g and h) in January and July of **2000**.

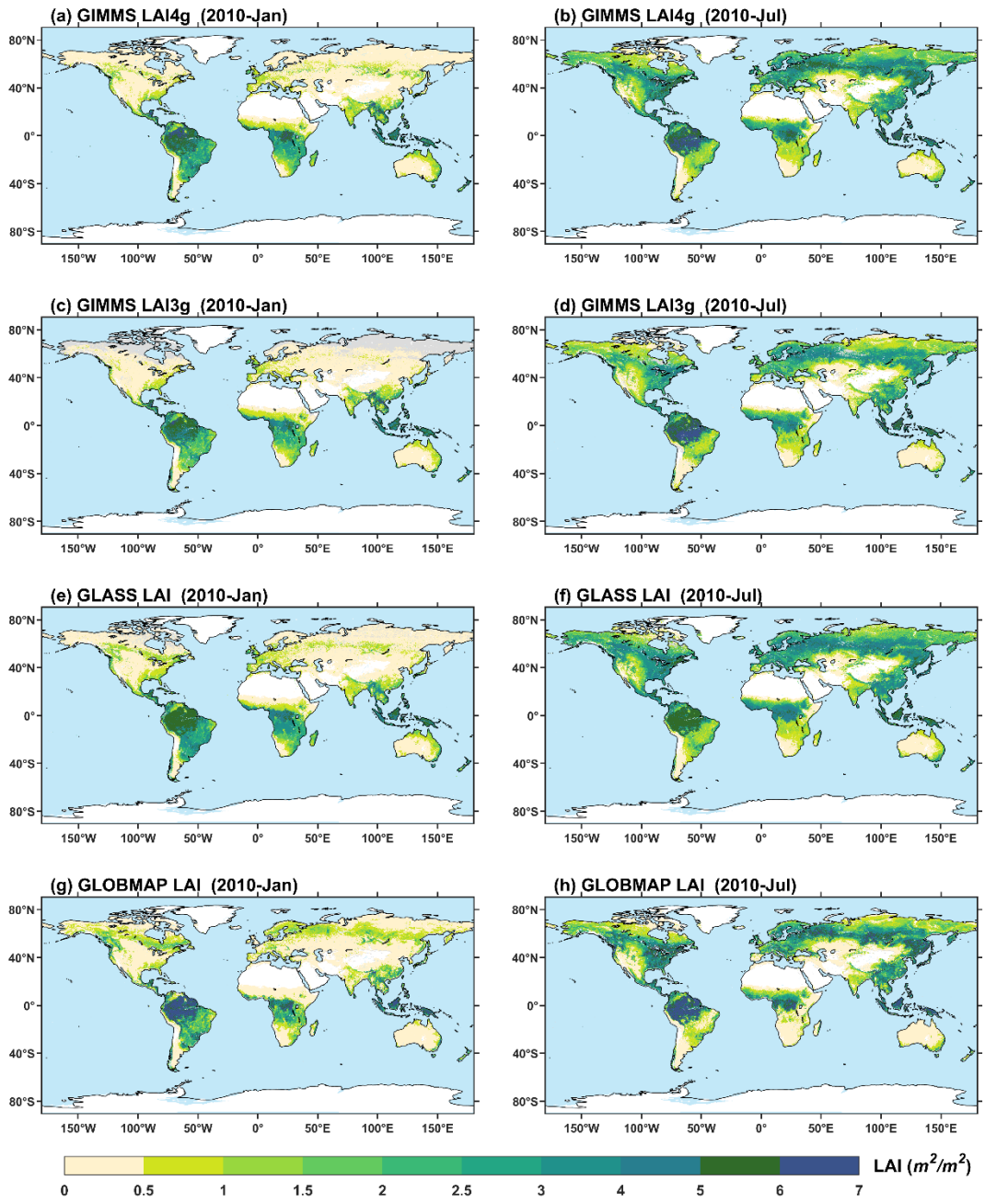

Figure S6. Illustrations of global distribution maps of GIMMS LAI4g after consolidation (a and b), GIMMS LAI3g (c and d), GLASS LAI (e and f), and GLOBMAP LAI (g and h) in January and July of **2010**.

The following changes are made in the revised manuscript:

- GIMMS LAI4g at representative time points in Section 4.3:

"The global distribution maps of LAI in January and July can be found in Figure S4−S6." (Page 20, Lines 422-423)

[Comment 8] *4. DIRECT 2.1 provides more field data and sites than this study used. Please add the quality control method for selecting "113 field LAI measurements from 49 sites".*

[Response 8] It is true that, DIRECT 2.1, together with BELMANIP 2.1 and ORNL, has much more field LAI measurements than those used in this study. For instance, DIRECT 2.1 presents 276 measurements from 172 sites. However, in terms of a spatial resolution of 1/12° and a temporal resolution of half-moth, the sites could be spatially (e.g., between Hailun_B and Hailun_C) and temporally overlapped (e.g., measurements on June 19th and 24th of 2012 at Honghe_D). In these cases, we averaged the measurements falling in the same spatial or temporal domain. On the other hand, BELMANIP 2.1 and DIRECT 2.1 provide 3 km × 3 km averaged LAI values and ORNL is site-based. The spatial mismatch between the global long-term LAI products and the field measurements could introduce uncertainties associated with geo-location errors and the scaling effect (Zhu et al., 2013). Thus, we carefully examined all the field LAI measurements and excluded those located in a heterogeneous landscape (i.e., different vegetation biome types) within an 8 km × 8 km window (approximately 1/12°).

The following changes are made in the revised manuscript:

- Introduction to field LAI measurements in section 2.8:

"We prudently examined all the measurements in BELMANIP 2.1, DIRECT 2.1, and ORNL, and removed those that were acquired from heterogeneous sites using an 8 km × 8 km window (approximately 1/12°). Redundant measurements among the three projects were also removed. In a spatial resolution of 1/12° and a temporal resolution of half-moth, we averaged the measurements falling in the same spatial or temporal domain." (Page 7, Lines 200-203)

References:

Berner, L. T., Massey, R., Jantz, P., Forbes, B. C., Macias-Fauria, M., Myers-Smith, I., Kumpula, T., Gauthier, G., Andreu-Hayles, L., Gaglioti, B. V., Burns, P., Zetterberg, P., D'Arrigo, R., and Goetz, S. J.: Summer warming explains widespread but not uniform greening in the Arctic tundra biome, Nat Commun, 11, 1-12, https://doi.org/10.1038/s41467-020-18479-5, 2020.

Ma, H. and Liang, S.: Development of the GLASS 250-m leaf area index product (version 6) from MODIS data using the bidirectional LSTM deep learning model, Remote Sens. Environ., 273, 112985, https://doi.org/10.1016/j.rse.2022.112985, 2022.

Zhu, Z., Bi, J., Pan, Y., Ganguly, S., Anav, A., Xu, L., Samanta, A., Piao, S., Nemani, R. R., and Myneni, R. B.: Global data sets of vegetation Leaf Area Index (LAI)3g and Fraction of Photosynthetically Active Radiation (FPAR)3g derived from Global Inventory Modeling and Mapping Studies (GIMMS) Normalized Difference Vegetation Index (NDVI3g) for the period 1981 to 2011, Remote Sens., 5, 927-948, https://doi.org/10.3390/rs5020927, 2013.

Zhu, Z., Wang, S. X., and Woodcock, C. E.: Improvement and expansion of the Fmask algorithm: cloud, cloud shadow, and snow detection for Landsats 4-7, 8, and Sentinel 2 images, Remote Sens Environ, 159, 269-277, https://doi.org/10.1016/j.rse.2014.12.014, 2015.